Trisubstituted Imidazoles as Mycobacterium tuberculosis Glutamine Synthetase Inhibitors

ARTICLE *in* JOURNAL OF MEDICINAL CHEMISTRY · MARCH 2012

Impact Factor: 5.45 · DOI: 10.1021/jm201212h · Source: PubMed

11 AUTHORS, INCLUDING:

Samir Yahiaoui
University Joseph Fourier - Grenoble 1
18 PUBLICATIONS **218** CITATIONS
SEE PROFILE

Martin Lindh
Uppsala University
5 PUBLICATIONS **82** CITATIONS
SEE PROFILE

Bachally Srinivasa
AstraZeneca
16 PUBLICATIONS **174** CITATIONS
SEE PROFILE

Sherry L Mowbray
Uppsala University
109 PUBLICATIONS **3,612** CITATIONS
SEE PROFILE

Journal of Medicinal Chemistry

Brief Article

pubs.acs.org/jmc

Trisubstituted Imidazoles as *Mycobacterium tuberculosis* Glutamine Synthetase Inhibitors†

Johan Gising,[‡,⊥] Mikael T. Nilsson,[§,⊥] Luke R. Odell,[‡] Samir Yahiaoui,[‡] Martin Lindh,[‡] Harini Iyer,[∥] Achyut M. Sinha,[∥] Bachally R. Srinivasa,[∥] Mats Larhed,[‡] Sherry L. Mowbray,[§] and Anders Karlén*[,‡]

[‡]Department of Medicinal Chemistry, Organic Pharmaceutical Chemistry, BMC, Uppsala University, Box 574, SE-751 23 Uppsala, Sweden

[§]Department of Cell and Molecular Biology, Structural Biology, BMC, Uppsala University, Box 596, SE-751 24 Uppsala, Sweden

[∥]AstraZeneca India Private Limited, Bellary Road, Hebbal, Bangalore 560024, India

Supporting Information

ABSTRACT: *Mycobacterium tuberculosis* glutamine synthetase (*Mt*GS) is a promising target for antituberculosis drug discovery. In a recent high-throughput screening study we identified several classes of *Mt*GS inhibitors targeting the ATP-binding site. We now explore one of these classes, the 2-*tert*-butyl-4,5-diarylimidazoles, and present the design, synthesis, and X-ray crystallographic studies leading to the identification of *Mt*GS inhibitors with submicromolar IC_{50} values and promising antituberculosis MIC values.

INTRODUCTION

Mycobacterium tuberculosis, the causative agent of tuberculosis, is one of the world's most deadly pathogens, leading to almost 1.7 million deaths annually despite more than 100 years of research.[1] Rapidly emerging drug-resistant and multidrug-resistant strains have provided additional impetus to the search for new therapeutic agents to combat the disease.[2,3] *M. tuberculosis* glutamine synthetase (*Mt*GS, EC 6.3.1.2) catalyzes the conversion of glutamate, ammonia, and ATP to glutamine, phosphate, and ADP.[4] *Mt*GS plays a key role in controlling the ammonia levels within infected host cells and so contributes to the pathogen's capacity to inhibit phagosome acidification and phagosome−lysosome fusion.[5,6] Furthermore, *Mt*GS is believed to be involved in cell wall biosynthesis; it is found extracellularly in large quantities, which is related to a role in the production of the poly-L-glutamate−glutamine that is a major component of the cell wall in pathogenic mycobacteria.[7] Treatment of *M. tuberculosis* with antisense oligonucleotides to GS mRNA[8] or with the GS inhibitor L-methionine-*S*-sulfoximine (MSO, **1**, Figure 1a)[9] inhibits biosynthesis of poly-L-glutamate−glutamine and the bacterial growth.[8,9]

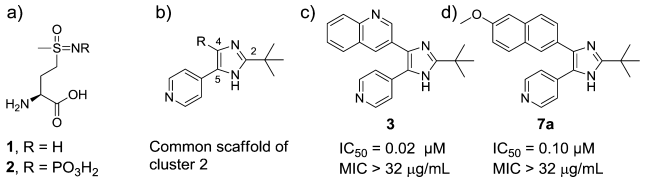

Figure 1. (a) Reference GS inhibitor **1** and phosphorylated transition-state analogue **2**. These two compounds bind to the amino acid-binding site of *Mt*GS. (b) Common scaffold of the HTS hits of cluster 2. (c, d) Two most potent compounds from cluster 2 in the HTS study. Compounds **3** and **7a** interact with the ATP-binding site of *Mt*GS.[12]

Compound **1** also shows in vivo efficacy in a guinea pig model, suggesting GS as a promising and druggable target in the treatment of *M. tuberculosis*.[10] The structure of *Mt*GS incubated with **1**, which is phosphorylated in situ to form the transition-state analogue L-methionine-*S*-sulfoximine phosphate (MSO-P, **2**, Figure 1a), has been reported showing how the inhibitor interacts in the amino acid binding site.[11]

In the present study we explore a new class of *Mt*GS inhibitors derived from a recent high throughput screening (HTS) study.[12,13] This screen targeted the ATP-binding site of *Mt*GS with the goal of moving away from the amino acid binding site,[14] which is largely conserved in human GS. The 2-*tert*-butyl-4-aryl-5-pyridylimidazole motif was the common structure in the hits assigned to cluster 2, with the 4-position substituted with various aryl groups (Figure 1b). From more than 20 compounds in this class, the two best were chosen for further SAR studies (**3** and **7a** in Figure 1c,d).

RESULTS AND DISCUSSION

We first sought a synthetic route to the two most active HTS hits in order to resynthesize them, confirm their activity, and initiate X-ray crystallographic studies. This proved to be problematic; despite exploration of various synthetic routes, we were never able to resynthesize **3**. However, the trisubstituted imidazole **7a** could be readily synthesized and was therefore used in the hit expansion of this cluster. The synthesis started from 2-bromo-6-methoxynaphthalene (**4**) with two consecutive Sonogashira couplings followed by an oxidation and cyclization to form the imidazole ring (see Scheme 1). The ethyne was introduced by a fast microwave assisted[15] Sonogashira method[16,17] using ethynyltrimethylsilane, dichlorobis(triphenylphosphine)palladium, copper iodide,

Received: September 13, 2011
Published: February 27, 2012

Scheme 1. Synthetic Route to Compounds 7a–m[a]

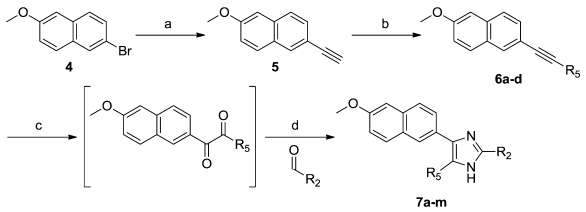

[a]Reagents and conditions: (a) ethynyltrimethylsilane, $Pd(PPh_3)_2Cl_2$, CuI, MeCN, diethylamine, microwave 120 °C, 15 min, then K_2CO_3, MeOH, rt, 2 h, 85%; (b) bromoaryl/heteroaryl, $Pd(PPh_3)_2Cl_2$, CuI, MeCN, diethylamine, microwave 80–120 °C, 15 min, 22–63%; (c) $KMnO_4$, phosphate buffer; (d) aldehyde, ammonium acetate, *n*-butanol, 50–65 °C, 0.5–5 h, 10–63%.

and acetonitrile/diethylamine (1:1) as solvent. In situ deprotection with saturated K_2CO_3 in methanol gave the 2-ethynyl-6-methoxynapthalene (**5**) in 85% yield. By use of the same protocol, the 4-pyridyl moiety was incorporated in moderate yield (**6a**, 47%). Oxidation of the ethyne **6a** to the diketone intermediate with potassium permanganate[18] in aqueous acetone proved to be a very sensitive reaction and often led to oxidative cleavage of the triple bond. Changing the standard buffer system $NaHCO_3/MgSO_4$ to NaH_2PO_4/Na_2HPO_4, and thus lowering the pH from 7.5 to 5, provided a more robust protocol to furnish the diketone. In our attempts to prepare **3**, the identical oxidation conditions with the corresponding quinoline intermediate only gave overoxidation, and no conditions were identified that suppressed oxidative cleavage. Finally the imidazole ring was synthesized by in situ trapping of the diketone with various aldehydes and ammonium acetate allowing straightforward variation of the *tert*-butyl group position (R2). The resynthesized HTS hit **7a** had IC_{50} = 3.1 μM, which is 30-fold higher than the IC_{50} obtained in the HTS study (0.1 μM), due to our more stringent assay conditions.[12] Unfortunately, neither **3** (from the AstraZeneca library) nor the resynthesized **7a** was active in the mycobacterial growth assay (MIC > 32 μg/mL).

Since numerous 4-substituted arylimidazoles of **7a** (Figure 1) had already been identified and evaluated in the HTS study, we focused instead on optimizing positions 2 (the *tert*-butyl group) and 5 (the 4-pyridyl group). The importance of the position of the nitrogen in the 4-pyridyl ring was first examined by synthesizing the phenyl and pyrimidine analogues (Table 1, **7b–d**). The same synthetic strategy as described above was applied, replacing the 4-pyridyl with aryl/heteroaryl groups introduced in the second Sonogashira reaction. Cyclization with pivalaldehyde gave the targets **7b–d** in which the nitrogen was either removed (**7b**) or its position altered (**7c–d**). The results clearly indicate the importance of having a nitrogen in the 4-position of the pyridine ring; all compounds lacking this feature were inactive (IC_{50} > 25 μM).

To investigate the importance of steric bulk in position 2 of the imidazole ring, compounds with smaller alkyl chains were synthesized. Cyclizing the diketone with propionaldehyde, acetaldehyde, and formaldehyde gave ethyl, methyl, and hydrogen, respectively, at position 2 of the imidazole ring (**7e–g** in Table 1). Removal of two methyl groups generated a slightly more active compound (**7e**, 2.2 μM vs **7a**, 3.1 μM). Removal of yet another methyl group yielded **7f**, which was inactive. Likewise, complete removal of the *tert*-butyl group

Table 1. Activities of Trisubstituted Imidazoles

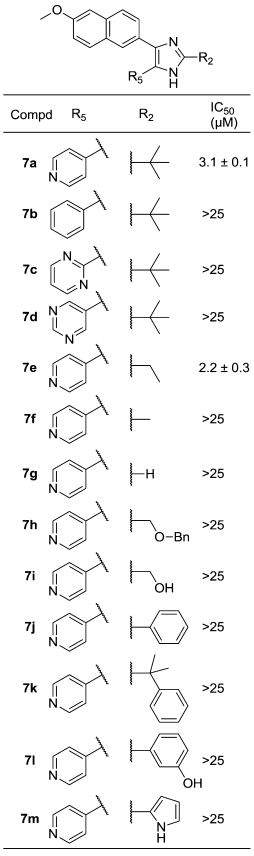

Compd	R_5	R_2	IC_{50} (μM)
7a	4-pyridyl	*t*-Bu	3.1 ± 0.1
7b	phenyl	*t*-Bu	>25
7c	3-pyridyl	*t*-Bu	>25
7d	2-pyrimidyl	*t*-Bu	>25
7e	4-pyridyl	Et	2.2 ± 0.3
7f	4-pyridyl	Me	>25
7g	4-pyridyl	H	>25
7h	4-pyridyl	CH$_2$OBn	>25
7i	4-pyridyl	CH$_2$OH	>25
7j	4-pyridyl	Ph	>25
7k	4-pyridyl	2-Me-Ph	>25
7l	4-pyridyl	3-OH-Ph	>25
7m	4-pyridyl	2-pyrrolyl	>25

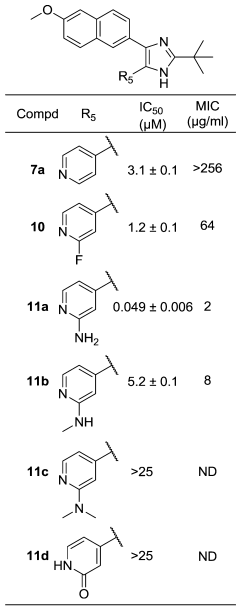

Compd	R_5	IC_{50} (μM)	MIC (μg/ml)
7a	4-pyridyl	3.1 ± 0.1	>256
10	3-F-4-pyridyl	1.2 ± 0.1	64
11a	2-NH$_2$-4-pyridyl	0.049 ± 0.006	2
11b	2-NH-4-pyridyl	5.2 ± 0.1	8
11c	2-N-4-pyridyl	>25	ND
11d	2-oxo-1,2-dihydro-4-pyridyl	>25	ND

ND = Not Determined

gave the inactive **7g**. Clearly, there is a preference for relatively bulky substituents in this position.

Parallel studies at this point produced the structure of *Mt*GS in complex with **2**, **3** (obtained from AstraZeneca's in-house compound library), phosphate, and magnesium at 2.15 Å resolution (crystallographic *R*-factor 22.5%, Figure 2a). An overlay of this structure on that of the complex with **2**, ADP, and magnesium (PDB entry 2BVC)[11] is shown in Figure 2b; an

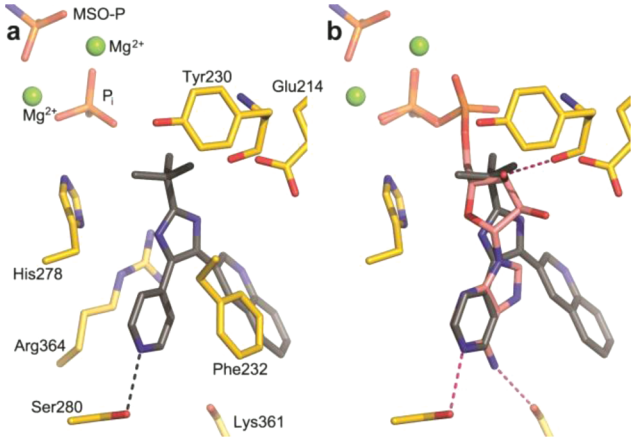

Figure 2. (a) *Mt*GS (yellow carbons) in complex with **2** (MSO-P), **3** (gray carbons), phosphate, and magnesium. Hydrogen bond between **3** and Ser280 is shown as a black dashed line. Nearby magnesium ions are green spheres. (b) Superposition of the *Mt*GS structure with **3** on that with bound ADP (PDB entry 2BVC) allows comparison to nucleotide (pink carbons) binding. Protein/ADP hydrogen bonds are pink dashed lines.

dx.doi.org/10.1021/jm201212h | *J. Med. Chem.* 2012, 55, 2894–2898

rmsd of 0.2 Å is obtained when the Cα's of residues 4−478 in the A chains are compared. Compound **2** occupies exactly the same position in the amino acid binding site in each case; all three of the metal ions are also in equivalent locations. The 4-pyridyl moiety of **3** is at essentially the same place as the six-membered pyrimidine ring of ADP, with the inhibitor's ring nitrogen providing the only hydrogen bond to protein (via the side chain of Ser280) in an interaction equivalent to that of N1 of ADP's adenine ring. The interaction with this serine explains why a nitrogen at the 4-position of the pyridine ring is so important for binding affinity (vide supra). The imidazole ring and *tert*-butyl moieties of **3** occupy roughly the same space as the ribose of the nucleotide. Thus, the R_2 group is found at the end of the ribose proximal to its linkage with the phosphates. A phosphate ion assumes the position of the β-phosphate of ADP. The quinoline moiety extends out toward the solvent, making van der Waals interactions with the protein only near Ala362 (not shown). Correspondingly, the electron density of this group is poorer than that of the rest of the ligand, although density in the maps averaged over all six subunits is clear (see Supporting Information). Efforts to cocrystallize **7a** with *Mt*GS were unsuccessful. However, we hypothesize that the binding modes of **3** and **7a** are very similar, which is supported by our docking studies. The comparisons in Figure 2b led us to make **7i**; docking studies indicated that the hydroxyl group of this compound could occupy the same position as O3′ of ADP and form an equivalent hydrogen bond to the backbone carbonyl of Tyr230 (Figure 2b). In the original synthetic route to **7i**, the hydroxyl was benzyl protected (**7h**) to ease the synthesis. However, all attempts to deprotect the corresponding alcohol by hydrogenation or oxidative protocols were unsuccessful. Compound **7h** was evaluated in the *Mt*GS assay but did not show any inhibitory activity at 25 μM. An alternative protective group strategy was then employed in which 2-(*tert*-butyldimethylsilyloxy)acetaldehyde was instead used in the imidazole ring cyclization. The silyloxy group allowed smooth deprotection with tetrabutylammonium fluoride to yield **7i**. Disappointingly, **7i** was also inactive in the enzymatic assay. The remaining compounds (**7j−m**) in Table 1 were similarly suggested to reach into the sugar-binding site of the ATP pocket. In the final step of the synthesis leading up to these compounds, aldehydes are used as reagents (see Scheme 1). We therefore created a set of virtual compounds by merging aldehydes found in-house and in the ACD database, using the Legion software.[19] The compounds were then docked to the nucleotide-binding site using Glide, and the fit was evaluated based on the Glide score and visual inspection. Despite their promising docking poses, **7j−m** all lacked inhibitory activity at 25 μM.

Going back to the superimposed X-ray structures, we decided to substitute the 4-pyridyl group of **7a** with a 2-aminopyridine-4-yl, which would possibly allow the formation of a hydrogen bond to the backbone carbonyl oxygen of Lys361, similar to the interaction seen for N6 of ADP (Figure 2b). Another synthetic approach was employed in the synthesis of the aminopyridines **11a−d**, avoiding the sensitive oxidation of the triple bond (Scheme 2). Ethyl 6-methoxy-2-naphthoate (**8**) was synthesized in 93% yield by a palladium-catalyzed carbonylation of 2-bromo-6-methoxynaphthalene (**4**) utilizing ethanol as the nucleophile.[20] In the next step, the fluorine of 2-fluoro-4-methylpyridine was incorporated as a handle to allow nucleophilic aromatic substitutions in later steps. Compound **9** was produced in acceptable yield (64%) by deprotonation of

Scheme 2. Synthetic Route to Compounds 11a−d[a]

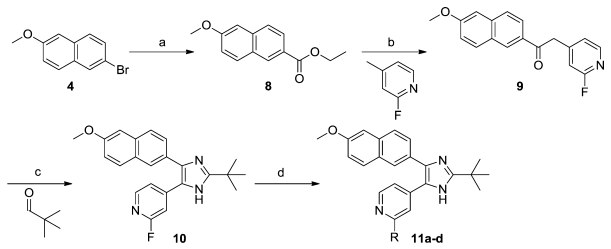

[a]Reagents and conditions: (a) EtOH, $Pd(OAc)_2$, Xantphos, DBU, $Mo(CO)_6$, microwave 120 °C, 30 min, 93%; (b) 2-fluoro-4-methylpyridine, NaHMDS, THF, 0 °C, 2 h, 64%; (c) HBr, DMSO, 70 °C, 2 h, then pivalaldehyde, ammonium acetate, *n*-butanol, 50 °C, 2 h, 71%. (d) **11a**: (i) diphenylmethanamine, dioxane, microwave 200 °C, 10 h, (ii) Pd/C, NH_4OAc, MeOH, microwave 120−140 °C, 2 h, 28%. **11b**: methylamine (2.0 M in THF), microwave 150 °C, 17 h, 18%. **11c**: ammonium hydroxide, DMF, microwave 150 °C, 12 h, 85%. **11d**: AcOH, H_2O, microwave 190 °C, 2 h, 91%.

2-fluoro-4-methylpyridine with NaHMDS via nucleophilic substitution of **8**. As an alternative to creating the imidazole ring from the diketone, an α-bromination was performed on **9** followed by cyclization with ammonium acetate and pivalaldehyde. Attempts to resynthesize the HTS hit **3** by this route again failed because we were never able to substitute the ethoxy of ethyl quinoline-3-carboxylate with 4-methylpyridine. At this point, it was encouraging to see that the fluorine in **10** contributed to an approximate 2.5-fold increase of affinity compared to the hit **7a** (IC_{50} of 1.2 μM vs 3.1 μM, Table 1). The aminopyridine **11a** was synthesized via microwave-assisted nucleophilic substitution of the fluorine of **10** with diphenylmethanamine followed by deprotection through catalytic hydrogenation. Remarkably, **11a** was over 60 times better than the reference **7a** (0.049 μM vs 3.1 μM, Table 1), suggesting an important new interaction with the enzyme. For comparison, the methylamino and the dimethylamino groups were incorporated in a similar way. Compound **11b**, having one methyl group, showed a 100-fold loss in activity compared to **11a**, making it even less potent than **7a**. Substituting the fluorine with a dimethylamino group resulted in **11c**, which was inactive. This suggested that having a hydrogen bond donating group in the 2-position of the pyridine ring was advantageous. As an alternative donating group, we introduced the 2-pyridone ring (**11d**), which we believed would bind in its 2-hydroxy tautomer. However, on the basis of the lack of activity of this compound, one can speculate that it predominantly exists in the pyridone form.

At this time, we succeeded in obtaining a crystal structure of **11a** bound to *Mt*GS together with **2**, phosphate, and magnesium at 2.26 Å resolution (*R*-factor 19.5%, Figure 3a). The complexes with **3** and **11a** are overlaid in Figure 3b; again, the protein structures are highly similar, with an rmsd of only 0.1 Å when the Cα's of residues 4−478 are compared. Ser280 of *Mt*GS was seen to interact with both nitrogens of the 2-aminopyridine-4-yl moiety of **11a** (only the hydrogen bond with the ring nitrogen was present in the complex with **3**), which shifts the ligand ∼0.5 Å deeper into the binding site. Inspection of the **11a** complex indicates that the distance is too great (∼3.5 Å) to support a hydrogen bond between the 2-amino group and the backbone carbonyl oxygen of Lys361. Apart from very small changes at the side chain of Phe232 and the main chain near residue Ala362, the protein structures are

dx.doi.org/10.1021/jm201212h | J. Med. Chem. 2012, 55, 2894−2898

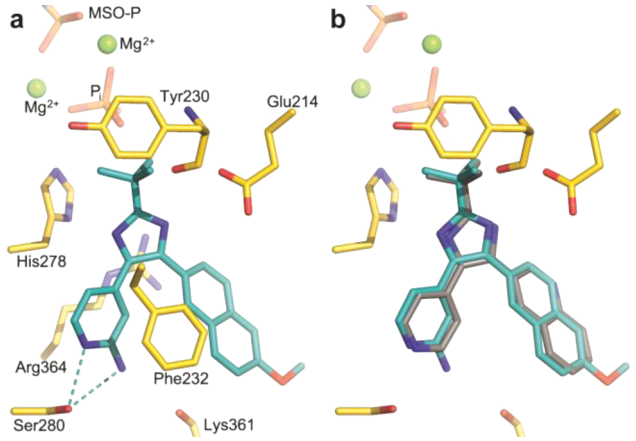

Figure 3. (a) *Mt*GS (yellow carbons) in complex with **2**, **11a** (cyan carbons), phosphate, and magnesium. Hydrogen bonds are shown as cyan dashed lines. (b) Superposition of the protein allows comparison of binding of **3** (gray carbons) and **11a**.

essentially identical. The compounds that inhibited *Mt*GS were also evaluated for their activity against the *M. tuberculosis* strain H37Rv. The hit **7a** and **7e** lacked antibacterial activity (MIC > 32 μg/mL), while the 2-pyridyl substituted compounds had promising MIC values; the most potent compound as measured by the enzymatic inhibition, **11a**, also gave the best MIC (2 μg/mL; see Table 1). To assess the potential cytotoxicity of **11a**, we performed a standard mammalian cell proliferation assay[22] using A549 cells; **11a** had an IC_{50} of 24.7 μm in this test, which is almost 5-fold greater than the MIC of 5.4 μM (2 μg/mL). This moderate level of cytotoxicity is not unusual among compounds in the early stages of drug development, and the situation is expected to improve as more effective enzyme inhibition and antibacterial activity are attained.

CONCLUSIONS

A recent HTS study targeting the ATP-binding site of *Mt*GS produced several active classes of compounds. One of these, the 2-*tert*-butyl-4,5-diarylimidazoles, contained several hits, and a complex with one of the inhibitors with *Mt*GS could be obtained by X-ray crystallography. On the basis of this structure, our initial SAR explorations could be rationalized as well as the importance of having a nitrogen, acting as a hydrogen bond acceptor, in the 4-position of the pyridine ring. Building out from the *tert*-butyl group, a series of compounds was designed to reach into the ribose-binding site of the ATP pocket. However, these compounds lacked inhibitory activity at 25 μM. An alternative synthetic strategy in which a 2-amino group was introduced into the 4-pyridyl ring was then pursued. This gave us our best inhibitor (**11a**) with IC_{50} = 0.049 μM on *Mt*GS and an MIC = 2 μg/mL against *M. tuberculosis*. We were also able to obtain an X-ray structure of this compound bound to *Mt*GS, which showed that instead of forming a hydrogen bond to the backbone carbonyl oxygen of Lys361 as predicted from docking studies, the 2-amino group formed an additional interaction with the hydroxyl oxygen of Ser280 in its primary binding mode.

EXPERIMENTAL PROCEDURES

General Methods. Microwave-assisted reactions were performed in sealed vials dedicated for microwave processing, using a Smith synthesizer. NMR spectra were recorded on a Varian Mercury Plus for ^{1}H at 399.9 MHz and for ^{13}C NMR at 100.5 MHz. Analytical HPLC–UV/MS analysis of pure products were performed on a Gilson HPLC system with a Chromolith SpeedROD RP-18e column (50 mm × 4.6 mm) equipped with a Finnigan AQA quadrupole mass spectrometer using a 4 mL/min CH_3CN/H_2O gradient (0.05% HCOOH) and detection by UV (DAD) and MS (ESI+). All compounds were determined to be >95% pure by HPLC–UV at 254 nm.

4-(2-*tert*-Butyl-4-(6-methoxynaphthalen-2-yl)-1*H*-imidazol-5-yl)pyridin-2-amine (11a). To a microwave vial (2–5 mL) were added **10** (50 mg, 0.13 mmol), diphenylmethanamine (1.5 mL), and dioxane (1.5 mL). The vial was then sealed under air and heated at 200 °C by microwave irradiation for 10 h. After cooling, the mixture was filtered through a plug of silica, eluted with EtOAc/isohexane (1:1) and the filtrate concentrated in vacuo. The crude mixture was then taken up in MeOH (2.0 mL) and transferred to a microwave vial (2–5 mL) loaded with Pd/C (10%, 5 mg) and ammonium acetate (100 mg, 1.3 mmol). The vial was then sealed under air and heated at 120 °C by microwave irradiation for 2 h. After the mixture was cooled, Pd/C (10%, 10 mg) and ammonium acetate (200 mg, 2.6 mmol) were added, and the mixture was heated by microwave irradiation for a further 20 min at 140 °C. After cooling, the mixture was diluted with EtOAc and saturated $NaHCO_3$ (10 mL each) and the two layers were separated. The aqueous layer was washed twice with EtOAc (10 mL), and the combined organic phases were concentrated in vacuo. The crude product was thereafter purified by silica column flash chromatography, eluting with EtOAc/methanol/triethylamine (1:0.05:0.01). Yield: 28%, 14 mg as a pale yellow solid. ^{1}H NMR ($CDCl_3$) δ 7.81 (d, J = 1.9 Hz, 1H), 7.72 (d, J = 8.6 Hz, 1H), 7.69 (m, 1H), 7.51 (dm, J = 6.1 Hz, 1H), 7.40 (dd, J = 8.6, 1.9 Hz, 1H), 7.16 (m, 1H), 7.14 (m, 1H), 6.91 (br s, 1H), 6.65 (dm, J = 6.1 Hz, 1H), 3.91 (s, 3H), 1.43, (s, 9H); ^{13}C NMR ($CDCl_3/CD_3OD$, 5:1) δ 170.3, 158.6, 157.4, 156.9, 146.6, 140.5, 134.5, 129.7, 128.9, 127.8, 127.6, 127.2, 126.4, 119.8, 111.7, 107.5, 106.0, 55.6, 33.2, 29.6 (one carbon signal was not detected).[21] ESI-MS (m/z) 373 (M + H$^+$). HRMS (M + H$^+$): 373.2037, $C_{23}H_{24}N_4O$ requires 373.2028.

ASSOCIATED CONTENT

Supporting Information

Additional experimental details concerning synthesis of all compounds, protein expression, purification, activity/inhibition studies, spectroscopic data, and structural studies. This material is available free of charge via the Internet at http://pubs.acs.org.

Accession Codes

[†]PDB codes for the *Mt*GS-**3** and *Mt*GS-**11a** structures are 3ZXR and 3ZXV, respectively.

AUTHOR INFORMATION

Corresponding Author

*Phone: +46-18-4714293. Fax: +46-18-4714474. E-mail: anders.karlen@orgfarm.uu.se.

Author Contributions

[⊥]J.G. and M.T.N. contributed equally to this work.

Notes

The authors declare no competing financial interest.

ACKNOWLEDGMENTS

We thank Johan Gustavsson for preparative work and Dr. Aleh Yahorau, Department of Pharmaceutical Biosciences, Uppsala University, Sweden, for conducting HRMS analyses. The Swedish Foundation for Strategic Research (SSF), the Swedish Research Council (VR), and the EU Sixth Framework Program NM4TB (Grant CT:018 923) provided financial support.

■ ABBREVIATIONS USED

*Mt*GS, glutamine synthetase from *Mycobacterium tuberculosis*; MIC, minimum inhibitory concentration; PDB, Protein Data Bank; WHO, World Health Organization; HTS, high throughput screening; MSO, L-methionine-*S*-sulfoximine; MSO-P, L-methionine-*S*-sulfoximine phosphate; MW, microwave

■ REFERENCES

(1) www.who.org.

(2) Raviglione, M. C.; Smith, I. M. XDR tuberculosis: implications for global public health. *N. Engl. J. Med.* **2007**, *356*, 656−659.

(3) Migliori, G. B.; Lange, C.; Centis, R.; Sotgiu, G.; Muetterlein, R.; Hoffmann, H.; Kliiman, K.; De laco, G.; Lauria, F. N.; Richardson, M. D.; Spanevello, A.; Cirillo, D. M.; Grp, T. S. Resistance to second-line injectables and treatment outcomes in multidrug-resistant and extensively drug-resistant tuberculosis cases. *Eur. Respir. J.* **2008**, *31*, 1155−1159.

(4) Liaw, S. H.; Eisenberg, D. Structural model for the reaction mechanism of glutamine synthetase, based on 5 crystal structures of enzyme substrate complexes. *Biochemistry* **1994**, *33*, 675−681.

(5) Gordon, A. H.; Darcyhart, P.; Young, M. R. Ammonia inhibits phagosome lysosome fusion in macrophages. *Nature* **1980**, *286*, 79−80.

(6) Clemens, D. L.; Horwitz, M. A. Characterization of the *Mycobacterium tuberculosis* phagosome and evidence that phagosomal maturation is inhibited. *J. Exp. Med.* **1995**, *181*, 257−270.

(7) Harth, G.; Clemens, D. L.; Horwitz, M. A. Glutamine-synthetase of *Mycobacterium tuberculosis*: extracellular release and characterization of its enzymatic-activity. *Proc. Natl. Acad. Sci. U.S.A.* **1994**, *91*, 9342−9346.

(8) Harth, G.; Zamecnik, P. C.; Tang, J. Y.; Tabatadze, D.; Horwitz, M. A. Treatment of *Mycobacterium tuberculosis* with antisense oligonucleotides to glutamine synthetase mRNA inhibits glutamine synthetase activity, formation of the poly-L-glutamate/glutamine cell wall structure, and bacterial replication. *Proc. Natl. Acad. Sci. U.S.A.* **2000**, *97*, 418−423.

(9) Harth, G.; Horwitz, M. A. An inhibitor of exported *Mycobacterium tuberculosis* glutamine synthetase selectively blocks the growth of pathogenic mycobacteria in axenic culture and in human monocytes: extracellular proteins as potential novel drug targets. *J. Exp. Med.* **1999**, *189*, 1425−1435.

(10) Harth, G.; Horwitz, M. A. Inhibition of *Mycobacterium tuberculosis* glutamine synthetase as a novel antibiotic strategy against tuberculosis: demonstration of efficacy in vivo. *Infect. Immun.* **2003**, *71*, 456−464.

(11) Krajewski, W. W.; Jones, T. A.; Mowbray, S. L. Structure of *Mycobacterium tuberculosis* glutamine synthetase in complex with a transition-state mimic provides functional insights. *Proc. Natl. Acad. Sci. U.S.A.* **2005**, *102*, 10499−10504.

(12) Nilsson, M. T.; Krajewski, W. W.; Yellagunda, S.; Prabhumurthy, S.; Chamarahally, G. N.; Siddamadappa, C.; Srinivasa, B. R.; Yahiaoui, S.; Larhed, M.; Karlén, A.; Jones, T. A.; Mowbray, S. L. Structural basis for the inhibition of *Mycobacterium tuberculosis* glutamine synthetase by novel ATP-competitive inhibitors. *J. Mol. Biol.* **2009**, *393*, 504−513.

(13) Odell, L. R.; Nilsson, M. T.; Gising, J.; Lagerlund, O.; Muthas, D.; Nordqvist, A.; Karlén, A.; Larhed, M. Functionalized 3-amino-imidazo[1,2-*a*]pyridines: a novel class of drug-like *Mycobacterium tuberculosis* glutamine synthetase inhibitors. *Bioorg. Med. Chem. Lett.* **2009**, *19*, 4790−4793.

(14) Nordqvist, A.; Nilsson, M. T.; Rottger, S.; Odell, L. R.; Krajewski, W. W.; Andersson, C. E.; Larhed, M.; Mowbray, S. L.; Karlén, A. Evaluation of the amino acid binding site of *Mycobacterium tuberculosis* glutamine synthetase for drug discovery. *Biorg. Med. Chem.* **2008**, *16*, 5501−5513.

(15) Larhed, M.; Hallberg, A. Microwave-assisted high-speed chemistry: a new technique in drug discovery. *Drug. Discovery Today.* **2001**, *6*, 406−416.

(16) Erdélyi, M.; Gogoll, A. Rapid homogeneous-phase Sonogashira coupling reactions using controlled microwave heating. *J. Org. Chem.* **2001**, *66*, 4165−4169.

(17) Wannberg, J.; Sabnis, Y. A.; Vrang, L.; Samuelsson, B.; Karlén, A.; Hallberg, A.; Larhed, M. A new structural theme in C-2-symmetric HIV-1 protease inhibitors: ortho-substituted P1/P1′ side chains. *Bioorg. Med. Chem.* **2006**, *14*, 5303−5315.

(18) Srinivasan, N. S.; Lee, D. G. Preparation of 1,2-diketones: oxidation of alkynes by potassium-permenganate in aqueous acetone. *J. Org. Chem.* **1979**, *44*, 1574−1574.

(19) *Legion*; Tripos: St. Louis, MO, 1998.

(20) Georgsson, J.; Hallberg, A.; Larhed, M. Rapid palladium-catalyzed synthesis of esters from aryl halides utilizing $Mo(CO)_6$ as a solid carbon monoxide source. *J. Comb. Chem.* **2003**, *5*, 350−352.

(21) Fedorov, L. A.; Savarino, P.; Viskardi, G.; Rebrov, A. I.; Barni, E. ^{13}C NMR spectroscopy of tautomeric conversions in imidazole compounds. *Russ. Chem. Bull.* **1992**, *41*, 223−230.

(22) O'Brien, J.; Wilson, I.; Orton, T.; Pognan, F. Investigation of the Alamar Blue (resazurin) fluorescent dye for the assessment of mammalian cell cytotoxicity. *Eur. J. Biochem.* **2000**, *267*, 5421−5426.